

# Catalytic Oxidation Properties and Characterization of $\text{LaSrCo}_{0.9}\text{B}'_{0.1}\text{O}_4$ ( $\text{B}' = \text{Mn, Fe, Ni, Cu}$ ) Mixed Oxides

Laitao LUO\*, Guangxin SHAO, Zhanhui DUAN  
*Institute of Applied Chemistry, Nanchang University,  
330047 Nanchang, P. R. CHINA  
e-mail: luolaitao@yahoo.com.cn*

Received 13.11.2004

Using a polyacrylamide gel method, a series of  $\text{LaSrCo}_{0.9}\text{B}'_{0.1}\text{O}_4$  ( $\text{B}' = \text{Mn, Fe, Ni, Cu}$ ) mixed oxides were prepared and their catalytic activity was studied with CO and  $\text{C}_3\text{H}_8$  oxidations as a testing reaction. The results show that the specific effects of  $\text{B}'$  ions on CO and  $\text{C}_3\text{H}_8$  oxidations depend on their category. In comparison to  $\text{LaSrCoO}_4$  catalyst, the activity of  $\text{LaSrCo}_{0.9}\text{Ni}_{0.1}\text{O}_4$  catalyst for CO and  $\text{C}_3\text{H}_8$  oxidations is higher, while only lower activity is obtained for Mn, Fe or Cu-doped catalysts. The information derived from TPD, XRD and iodometry experiments shows that the increase in oxidation activity of  $\text{LaSrCo}_{0.9}\text{Ni}_{0.1}\text{O}_4$  catalyst towards CO and  $\text{C}_3\text{H}_8$  oxidation can be related to the increases in  $\text{O}_2$ -adsorption quantity,  $\text{CO}_2$ -desorption quantity, oxygen vacancies and lattice distortion due to the adulteration of nickel. Further investigation shows that the apparent activation energy of  $\text{LaSrCo}_{0.9}\text{Ni}_{0.1}\text{O}_4$  towards CO oxidation is lower than that of  $\text{LaSrCoO}_4$ .

**Key Words:** B-site adulteration, catalytic oxidation, Co-based mixed oxides,  $\text{A}_2\text{BO}_4$ .

## Introduction

Perovskite-like  $\text{A}_2\text{BO}_4$  mixed oxides, with a  $\text{K}_2\text{NiF}_4$ -type structure, have attracted more and more attention in the catalysis field because of their unique features, such as low cost, high catalytic activity and excellent thermal stability<sup>1,2</sup>. Many studies have shown that the catalytic performances of  $\text{A}_2\text{BO}_4$  mixed oxides, to a large extent, are associated with the species of A-site and B-site ions, and their corresponding valences, as well as the crystal structure of these oxides<sup>3-5</sup>. As commonly accepted, B-site ions, i.e. framework ions, can play important roles in determining catalytic activity. It is noted that there are many studies in the literature on investigations of  $\text{LaSrCuO}_4$  and  $\text{LaSrNiO}_4$  catalysts<sup>2-3,6-9</sup>. Recently, it was reported<sup>10,11</sup> that in some catalytic oxidation reactions  $\text{LaSrCoO}_4$  catalyst shows excellent performance. Studies involving the investigation of  $\text{LaSrCoO}_4$  catalyst are considerably limited. Furthermore, almost no research has been dedicated to the adulteration of B-site ions in such catalysts, although the adulteration in the B-site is promising. Therefore, further investigation is necessary.

---

\*Corresponding author

Four ions (Mn, Fe, Ni, Cu) in the present case are introduced into LaSrCoO<sub>4</sub> catalyst and one of main purposes is to discuss the specific role of B-site doped-ions in catalysis. With CO and C<sub>3</sub>H<sub>8</sub> oxidations as testing reactions, the catalytic performances of all these catalysts were investigated. To show the probable intrinsic properties, XRD, TEM and TPD were employed.

## Experimental

### Preparations of LaSrCoO<sub>4</sub> and LaSrCo<sub>0.9</sub>B'<sub>0.1</sub>O<sub>4</sub> (B=Mn, Fe, Ni, Cu) catalysts

The mixed oxides were prepared by the polyacrylamide-gel method<sup>3</sup>. Under stirring, a certain molar ratio of lanthanum, strontium, cobalt and manganese (or iron, nickel, copper) in salt nitrate forms were dissolved in a citric solution. At pH 6-7 (ammonia adjustor), acrylamide and *N, N'*-methylene-bis-acrylamide were added, and then the system was heated to 90~95 °C. Subsequently, *N, N, N', N'*-tetramethylethylenediamine and 2,2'-azo-bis-iso-butyronitrile (dissolved in ethanol) were added as initiators and the resulting gel was dried by evaporation. With the temperature-increasing rate of 2 °C·min<sup>-1</sup>, the obtained precursor was heated to 450 °C and left for 6 h, followed by calcination at 850 °C for 9 h.

### Catalytic activity measurements

The CO and C<sub>3</sub>H<sub>8</sub> oxidation reaction was carried out with a flow reactor. For each experiment, 0.2 g of catalyst was used. The space velocity was 6000 h<sup>-1</sup> and the composition of the mixture gases was CO, 3.5%-vol, C<sub>3</sub>H<sub>8</sub>, 1.0%-vol, O<sub>2</sub>, 7.0% -vol and N<sub>2</sub>, 88.5%-vol. For the determination of the conversions of CO and C<sub>3</sub>H<sub>8</sub>, evaluating the activity of catalyst, on-line chromatography with a TCD detector was used. For the analysis of CO oxidation, the separation column was TDX-01 and a Porapak Q column was used for C<sub>3</sub>H<sub>8</sub> oxidation.

### XRD measurement

The XRD analysis was carried out on an X-ray diffractometer (D/max-3B, Japan), with the operation conditions as 40 kV/10 mA, Cu K $\alpha$  and nickel filter.

### Valence analysis of B-site ions

The valence of B-site ions was determined by means of iodometry<sup>12</sup>.

### TPD characterizations

O<sub>2</sub>-TPD or CO<sub>2</sub>-TPD: under O<sub>2</sub> or CO<sub>2</sub> gas, a catalyst sample (250 mg) was heated from ambient temperature to 800 °C (500 °C for CO<sub>2</sub>-TPD) at a rate of 10 °C ·min<sup>-1</sup> and subsequently left for 1 h. When the system was cooled to room temperature, He (carrier gas) was used to remove the O<sub>2</sub> or CO<sub>2</sub> in the gas-phase. Subsequently, with the temperature-increasing rate of 8 °C·min<sup>-1</sup>, the O<sub>2</sub> or CO<sub>2</sub>-desorption was recorded by on-line chromatography.

## Results and Discussion

### Catalytic oxidation activity of $\text{LaSrCoO}_4$ and $\text{LaSrCo}_{0.9}\text{B}'_{0.1}\text{O}_4$ catalysts

Table 1 and Figure 1 show the oxidation activity of various catalysts. Here,  $T_{50}$  and  $T_{100}$  are the temperatures of CO and  $\text{C}_3\text{H}_8$  conversions reaching 50% and 100%, respectively. As is apparent, the oxidation activity of  $\text{LaSrCo}_{0.9}\text{Ni}_{0.1}\text{O}_4$  catalyst is higher than that of  $\text{LaSrCoO}_4$ , while only lower activity is obtained for Fe, Mn or Cu doped-catalysts than for  $\text{LaSrCoO}_4$ . In comparison to  $\text{LaSrCoO}_4$ ,  $T_{50}$  and  $T_{100}$  of CO oxidation of  $\text{LaSrCo}_{0.9}\text{Ni}_{0.1}\text{O}_4$  are decreased respectively 15 and 10 °C. Both decreases become more evident in the case of  $\text{C}_3\text{H}_8$  oxidation. This strongly indicates that the presence of B-site adulteration plays an important role in affecting the catalytic activity. In comparison to the lowest  $T_{100}$  (350 °C) of CO oxidation over  $\text{La}_{2-x}\text{Sr}_x\text{NiO}_4$  ( $x=0-1.0$ ) and  $\text{Eu}_{2-x}\text{Sr}_x\text{CuO}_4$  ( $x=0-0.6$ ) reported in the literature<sup>7,13</sup>, the case of  $\text{LaSrCo}_{0.9}\text{Ni}_{0.1}\text{O}_4$  catalyst presents lower  $T_{100}$  (220 °C). This indicates that  $\text{LaSrCo}_{0.9}\text{Ni}_{0.1}\text{O}_4$  is a better oxidation-typed catalyst.

**Table 1.** Effect of doped-ions on the catalytic activity of  $\text{LaSrCo}_{0.9}\text{B}'_{0.1}\text{O}_4$  mixed oxides towards CO and  $\text{C}_3\text{H}_8$  oxidation.

Catalysts	CO Oxidation		$\text{C}_3\text{H}_8$ Oxidation	
	$T_{50}/^\circ\text{C}$	$T_{100}/^\circ\text{C}$	$T_{50}/^\circ\text{C}$	$T_{100}/^\circ\text{C}$
$\text{LaSrCoO}_4$	208	230	321	375
$\text{LaSrCo}_{0.9}\text{Fe}_{0.1}\text{O}_4$	217	250	354	410
$\text{LaSrCo}_{0.9}\text{Ni}_{0.1}\text{O}_4$	194	220	303	350
$\text{LaSrCo}_{0.9}\text{Cu}_{0.1}\text{O}_4$	223	250	367	455
$\text{LaSrCo}_{0.9}\text{Mn}_{0.1}\text{O}_4$	211	230	324	380

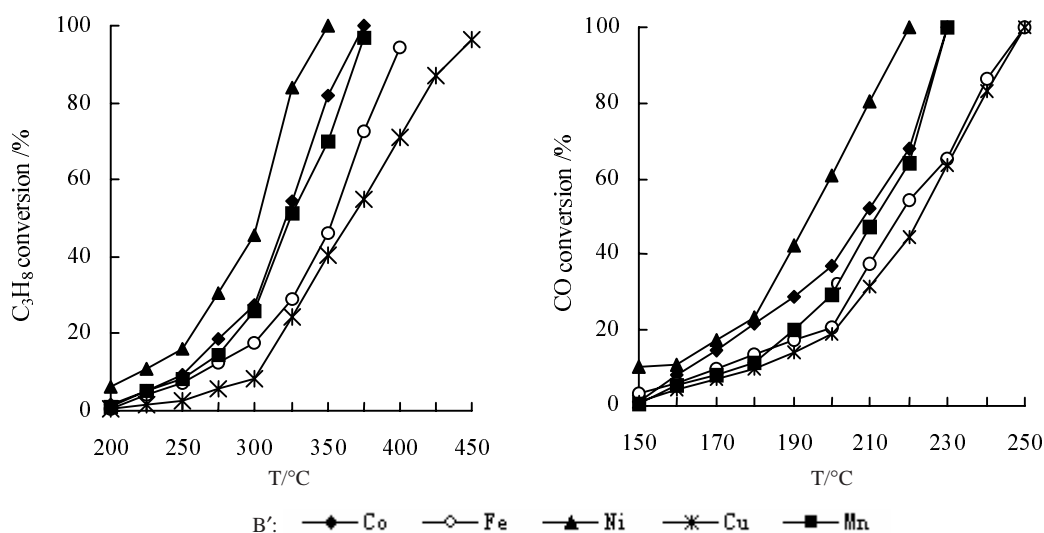


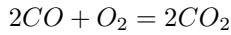
**Figure 1.** Effect of reaction temperature on the catalytic activity of  $\text{LaSrCoO}_4$  and  $\text{LaSrCo}_{0.9}\text{B}'_{0.1}\text{O}_4$  ( $\text{B}' = \text{Mn, Fe, Ni, Cu}$ ) catalysts.

As also noted, the oxidation temperature of  $\text{C}_3\text{H}_8$  is actually higher than that of CO. This may be due to the higher C-H and C-C bond-energy ( $411 \text{ kJ}\cdot\text{mol}^{-1}$ ,  $345.6 \text{ kJ}\cdot\text{mol}^{-1}$ ) than  $\pi$  bond-energy ( $273$

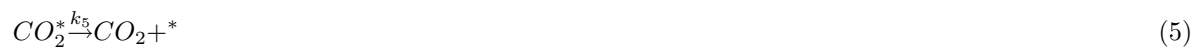
$\text{kJ}\cdot\text{mol}^{-1}$ ) held in CO. As a result, opening a bond in  $\text{C}_3\text{H}_8$  would need higher energy than in CO molecule and therefore a higher oxidation temperature for  $\text{C}_3\text{H}_8$  oxidation than for CO oxidation is obtained.

### Studies on apparent activation energy towards CO oxidation

Activation energy indicates that a reaction is hard or easy and to what extent. The nature of catalysts' increasing reaction speed is that catalysts decrease the activation energy. The CO oxidation is such that CO reacts with  $\text{O}_2$  to form  $\text{CO}_2$ , and the reaction equation is



The mechanism of CO oxidation is discovered through Doden's research:



The surface reaction is the speed-control step, and equations can be drawn when other steps come to balance:

$$k_1 P_{\text{CO}} \theta_0 = k_{-1} [\text{CO}^*] \quad (6)$$

$$k_2 P_{\text{O}_2} \theta_0 = k_{-2} [\text{O}_2^*] \quad (7)$$

$$k_3 [\text{O}_2^*] \theta_0 = k_{-3} [\text{O}^*]^2 \quad (8)$$

The speed of the surface reaction is

$$r = k_4 [\text{CO}^*] [\text{O}^*] \quad (9)$$

Import Equations of [6], [7] and [8] to equation [9]

$$r = -\frac{dP}{dt} = k_4 \frac{k_1 P_{\text{CO}} \theta_0}{k_{-1}} \sqrt{\frac{k_3 k_2 P_{\text{O}_2} \theta_0^2}{k_{-2} k_{-3}}} = K P_{\text{CO}} P_{\text{O}_2}^{1/2} \theta_0^2 \quad (10)$$

From the equation above, it can be seen that CO oxidation is a 3/2 grade reaction. Oxygen is abundant in the reaction condition, and so partial pressure of oxygen and the quantity of free adsorption center are thought to be invariable when the reaction comes to balance. Thus equation [10] can be written as

$$r = -dP/dt = A e^{-E_a/RT} \cdot P_{\text{CO}} \cdot C$$

$$-\int \frac{1}{P_{CO}} dP = \int A e^{-E_a/RT} \cdot C \cdot dt$$

$$-\ln \frac{P}{P_0} = A e^{-E_a/RT} \cdot t + C' \quad (11)$$

Because the gas-space velocity and the catalyst quantity are the same in the reaction process, the time spent by the gas that passes through the catalyst bed should be the same, and it is a constant. The total gas pressure is regarded as invariable due to plentiful diluting gas in the mixed reaction gas. Thus, CO conversion  $X=(P_0-P)/P_0$ .

$$\ln \ln \frac{1}{1-X} = -E_a/RT + C'' \quad (12)$$

From equation [12], figures of  $\ln \ln \frac{1}{1-X}$  vs.  $1/T$  can be drawn, and the apparent activation energy towards CO oxidation can be obtained from the slope ( $-E_a/R$ ).

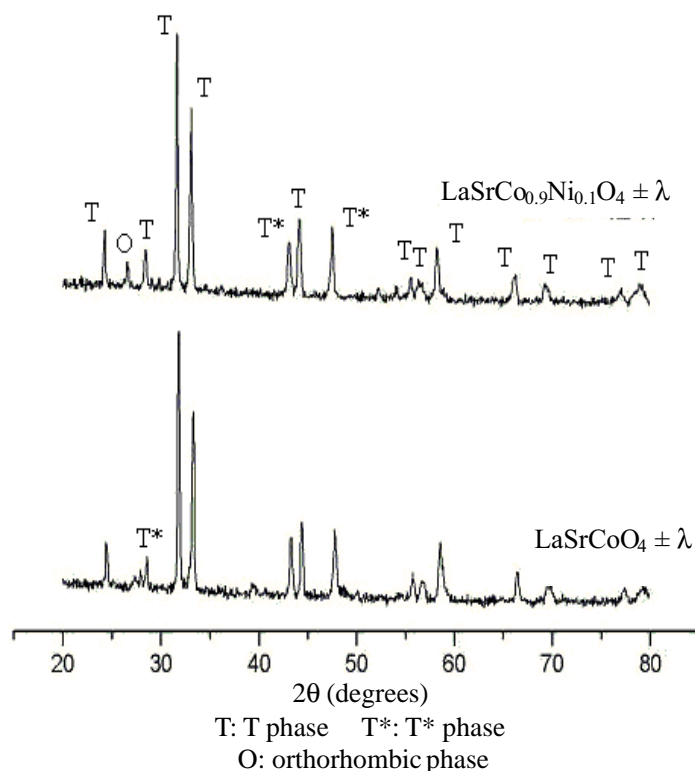
The apparent activation energy of  $\text{LaSrCoO}_4$  and  $\text{LaSrCo}_{0.9}\text{Ni}_{0.1}\text{O}_4$  is shown in Table 2. In comparison to  $\text{LaSrCoO}_4$ , the apparent activation energy of  $\text{LaSrCo}_{0.9}\text{Ni}_{0.1}\text{O}_4$  is lower by  $11.8 \text{ kJ}\cdot\text{mol}^{-1}$ . Because of the speed constant  $K=Ae^{-E_a/RT}$ , the less the activation energy ( $E_a$ ) is, the greater the speed constant is, and the faster the reaction is with high catalytic activity, which hits the experiment results.

**Table 2.** Apparent activation energy towards CO oxidation.

Samples	Activation energy / $\text{kJ}\cdot\text{mol}^{-1}$
$\text{LaSrCoO}_4$	153.7
$\text{LaSrCo}_{0.9}\text{Ni}_{0.1}\text{O}_4$	141.9

## Structural characterizations of $\text{LaSrCoO}_4$ and $\text{LaSrCo}_{0.9}\text{Ni}_{0.1}\text{O}_4$ catalysts

As is well known, the formation of  $\text{K}_2\text{NiF}_4$ -typed  $\text{A}_2\text{BO}_4$  mixed oxides has 2 aspects of requirements, that is, the limitation of structure factor  $t$  ( $R_A/R_B=1.7\sim 2.4$ ) and the requirement of charge balance<sup>14,15</sup>. Since the 2 aspects of have been met,  $\text{LaSrCoO}_4$  and  $\text{LaSrCo}_{0.9}\text{Ni}_{0.1}\text{O}_4$  can form  $\text{K}_2\text{NiF}_4$ -typed structure under appropriate conditions. It is also known that  $\text{K}_2\text{NiF}_4$ -typed  $\text{A}_2\text{BO}_4$  mixed oxides can be classified specially into 2 forms, i.e. space group  $Fmmm$  orthorhombic-phase and space group  $I4/mmm$  tetragonal-phase; also the  $I4/mmm$  tetragonal-phase of  $\text{A}_2\text{BO}_4$  can be classified further into 3 phases (T, T\*, T')<sup>16</sup>. B-site ions are coordinated with 6, 5 and 4 oxygen atoms ( $\text{BO}_6$ ,  $\text{BO}_5$  and  $\text{BO}_4$ ) in T, T\* and T' phases, respectively. The results of the XRD pattern (Figure 2) clearly indicate that both  $\text{LaSrCoO}_4$  and  $\text{LaSrCo}_{0.9}\text{Ni}_{0.1}\text{O}_4$  show a  $\text{K}_2\text{NiF}_4$  structure, which consists of a T phase and a small T\* phase. Moreover,  $\text{LaSrCo}_{0.9}\text{Ni}_{0.1}\text{O}_4$  also contains less orthorhombic phase.



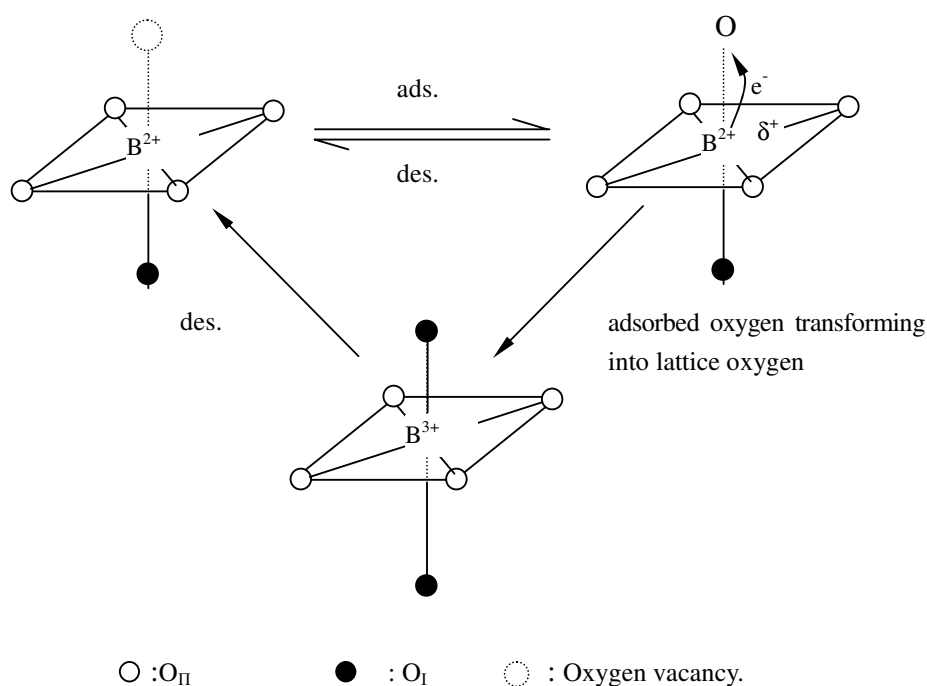
**Figure 2.** XRD patterns of the  $\text{LaSrCo}_{0.9}\text{Ni}_{0.1}\text{O}_4$  and  $\text{LaSrCoO}_4$  mixed oxides.

Figure 3 shows the schemes of oxygen transformation in the octahedral  $\text{BO}_6$  over  $\text{LaSrCo}_{0.9}\text{B}'_{0.1}\text{O}_4$  catalysts in the reaction of CO and  $\text{C}_3\text{H}_8$  oxidation<sup>17</sup>. Here,  $\text{BO}_6$ , the activity unit of  $\text{LaSrCo}_{0.9}\text{B}'_{0.1}\text{O}_4$  catalysts, is a distorted octahedron. In  $\text{BO}_6$ , the B- $\text{O}_\text{I}$  bond-length is longer than that of B- $\text{O}_\text{II}$ . For catalytic oxidation, the  $\text{O}_\text{I}$  that connects with the high-valence B-site ions plays an important role in the catalytic oxidation. In the process of oxidation, CO and  $\text{C}_3\text{H}_8$  are adsorbed to the high-valence B-site ions and subsequently activated, followed by their reaction with  $\text{O}_\text{I}$ .

As commonly accepted<sup>3,9</sup>, the distortion of the active unit  $\text{BO}_6$ , caused by different B-site ions or B-site doped ions, is an important reason for the different activity. For evaluations of average crystal size and lattice distortion, the Scherrer equation  $L=0.9\lambda/\beta\cos\theta$  and  $\beta^2\cos^2\theta=4(\lambda/L)^2/\pi^2+32(\varepsilon^2)\text{Sin}^2\theta$  were used. Here, L is the average crystal size,  $\lambda$  the X-ray wavelength used (0.1542 nm),  $\beta$  the half-peak width,  $\theta$  the diffraction angle and  $(\varepsilon^2)^{1/2}$  the lattice distortion. In the direction of [110] and [103], the results (Table 3) show that the crystal size of  $\text{LaSrCo}_{0.9}\text{Ni}_{0.1}\text{O}_4$  is smaller than that of  $\text{LaSrCoO}_4$ ; also the lattice distortion is actually greater. The increase in lattice distortion will increase the B- $\text{O}_\text{I}$  bond-length and decrease B- $\text{O}_\text{II}$  bond-length ( $\text{O}_\text{I}$ : oxygen in c lattice axis;  $\text{O}_\text{II}$ : oxygen in x-y lattice plane). As a result, the mobility of  $\text{O}_\text{I}$  will increase, which is beneficial to the process of oxidation reaction<sup>18,19</sup>.

**Table 3.** Average crystal size and lattice distortion of the  $\text{LaSrCoO}_4$  and  $\text{LaSrCo}_{0.9}\text{Ni}_{0.1}\text{O}_4$  mixed oxides.

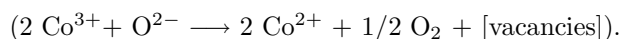
Mixed oxides	$L_{110}/\text{nm}$	$(\varepsilon^2)_{110}^{1/2}/10^{-3}$	$L_{103}/\text{nm}$	$(\varepsilon^2)_{103}^{1/2}/10^{-3}$
$\text{LaSrCoO}_4$	39.32	1.61	32.23	1.88
$\text{LaSrCo}_{0.9}\text{Ni}_{0.1}\text{O}_4$	33.31	1.91	31.76	1.92



**Figure 3.** Schemes of oxygen transformation in the octahedral BO<sub>6</sub>.

### TPD Characterizations of LaSrCoO<sub>4</sub> and LaSrCo<sub>0.9</sub>Ni<sub>0.1</sub>O<sub>4</sub> catalysts

O<sub>2</sub>-TPD curves of LaSrCoO<sub>4</sub> and LaSrCo<sub>0.9</sub>Ni<sub>0.1</sub>O<sub>4</sub> catalysts are shown in Figure 4. There are 3 peaks (i.e.  $\alpha$ ,  $\alpha'$  and  $\beta$ ) in the desorption curve of LaSrCoO<sub>4</sub> catalyst. The peak  $\alpha$  may be due to the desorbing of the ordinarily chemically adsorbed oxygen on the surface of the catalyst, while the peak  $\alpha'$  may be related to the chemically adsorbed oxygen in the oxygen vacancies of the catalyst<sup>20</sup>. The release of oxygen vacancies may be due to the reduction of Co<sup>3+</sup>:



The peak  $\beta$  responds to the release of oxygen in the lattice of the catalyst. For LaSrCo<sub>0.9</sub>Ni<sub>0.1</sub>O<sub>4</sub> catalyst, there are some differences in the curve, that is, another peak (i.e.  $\alpha^*$ ) appearing in the TPD curve. This is probably due to the presence of 2 different oxygen vacancies, since the B-site ions contain not only Co but also Ni. Thus, logically, the peak  $\alpha'$  and  $\alpha^*$  may be responsible for the reduction of Co<sup>3+</sup> ions and Ni<sup>3+</sup> ions with the release of oxygen vacancies.

As can also be seen from Figure 4, the ordinarily chemically adsorbed oxygen and the chemically adsorbed oxygen on oxygen vacancies of LaSrCo<sub>0.9</sub>Ni<sub>0.1</sub>O<sub>4</sub> are more those that of LaSrCoO<sub>4</sub>.

Since CO<sub>2</sub> is the product of CO and C<sub>3</sub>H<sub>8</sub> full-oxidation, the investigation of CO<sub>2</sub>-TPD is necessary, and this may reveal some information about the oxidation. As shown in Figure 5, there are 2 CO<sub>2</sub>-desorption peaks in the TPD curves of both LaSrCoO<sub>4</sub> and LaSrCo<sub>0.9</sub>Ni<sub>0.1</sub>O<sub>4</sub>, while the bigger area desorbed is under the curve of LaSrCo<sub>0.9</sub>Ni<sub>0.1</sub>O<sub>4</sub>. This indicates that a larger empty position on the surface of the catalyst can be left, therefore giving more room for subsequent reactions, which is beneficial to the reaction.

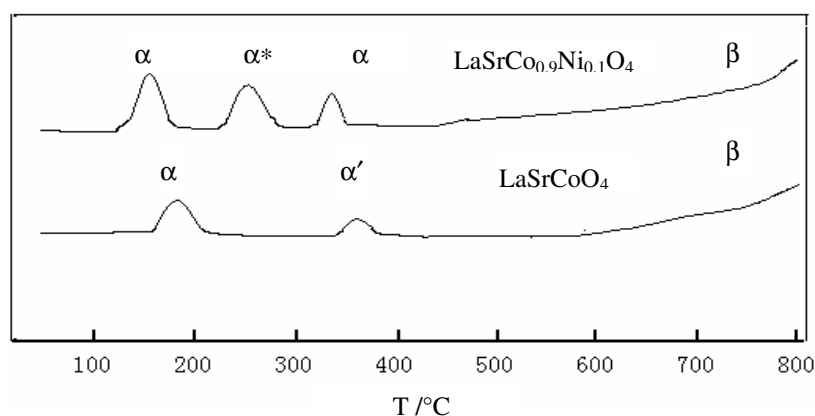


Figure 4. O<sub>2</sub>-TPD curves of the LaSrCoO<sub>4</sub> and LaSrCo<sub>0.9</sub>Ni<sub>0.1</sub>O<sub>4</sub> mixed oxides.

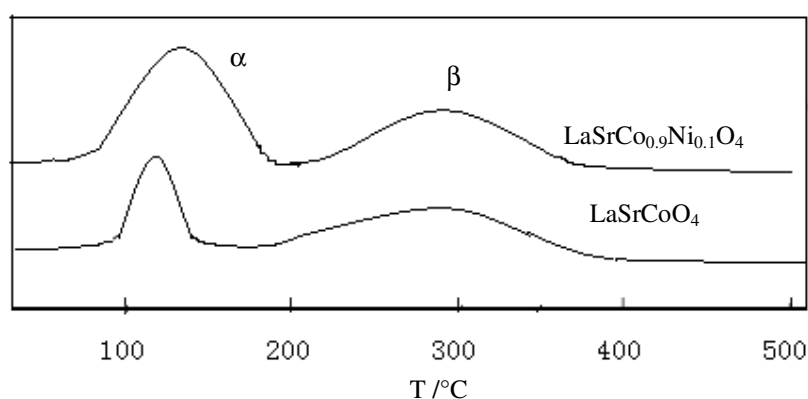


Figure 5. CO<sub>2</sub>-TPD curves of the LaSrCoO<sub>4</sub> and LaSrCo<sub>0.9</sub>Ni<sub>0.1</sub>O<sub>4</sub> mixed oxides.

### Valence of B-site ions and non-stoichiometric oxygen analysis

The iodometry experiments show that the average valence of B-site ions in LaSrCoO<sub>4</sub> and LaSrCo<sub>0.9</sub>Ni<sub>0.1</sub>O<sub>4</sub> is 2.323 and 2.226, respectively. In addition, the content of their non-stoichiometric oxygen is 0.339 and 0.387, respectively, indicating that oxygen vacancies of LaSrCo<sub>0.9</sub>Ni<sub>0.1</sub>O<sub>4</sub> increase. As mentioned above, the oxygen vacancies play an important role in the catalytic oxidation reaction. During the catalytic oxidation, these oxygen vacancies, on one hand, aid in the transformation of the chemisorbed oxygen to the lattice oxygen continuously, thereby supplementing the consumption of lattice oxygen, and, on the other hand, also increase the mobility of lattice oxygen, as well as produce more lattice oxygen. As a result, the activity of LaSrCo<sub>0.9</sub>Ni<sub>0.1</sub>O<sub>4</sub> catalyst is reinforced.

### Conclusions

A series of perovskite-like LaSrCo<sub>0.9</sub>B'<sub>0.1</sub>O<sub>4</sub> (B' = Mn, Fe, Ni, Cu) mixed oxides, in nanometer size, were prepared by polyacrylamide gel method. The results show that the specific effects of B' ions on CO and C<sub>3</sub>H<sub>8</sub> oxidations depend on their category. In comparison to LaSrCoO<sub>4</sub> catalyst, the activity of LaSrCo<sub>0.9</sub>Ni<sub>0.1</sub>O<sub>4</sub> catalyst is higher, while only lower activity is obtained for Mn, Fe or Cu-doped catalysts. Further information shows that the increase the activity may be related to the increases in O<sub>2</sub>-adsorption quantity, CO<sub>2</sub>-desorption quantity, oxygen vacancies and the lattice distortion due to the adulteration of nickel. In addition, the apparent activation energy of LaSrCo<sub>0.9</sub>Ni<sub>0.1</sub>O<sub>4</sub> towards CO oxidation is lower than that of LaSrCoO<sub>4</sub>.

## Acknowledgments

The authors thank Dr. Songjun Li for the valuable discussions on this work.

## References

1. N. Guilhaume, S.D. Peter and M. Primet, **Appl. Catal. B.** **10**, 325-344 (1996).
2. S.D. Peter, E. Garbowski, N. Guilhaume, V. Perrichon and M. Primet, **Catal. Lett.** **54**, 79-84 (1998).
3. Y. Liu, X.G. Yang, Y.M. Liu and Y. Wu, **Acta Phys.-chim. Sin.** **15**, 506-511 (1999).
4. L.Z. Gao, Q.S. Li, Y. Wu and Z.L. Yu, **Acta Chim. Sin.** **54**, 234-241 (1996).
5. Z. Zhao, X.G. Yang and Y. Wu, **Acta Phys.-chim. Sin.** **13**, 344-350 (1997).
6. A.K. Ladavos and P.J. Pomonis, **Appl. Catal. A**, **165**, 73-85 (1997).
7. H. Lou, H.Y. Zhen, J.Y. Yang, Z.Q. Yao, X. Yu, S.B. Du and F.T. Ma, **Chem. J. Chinese U.** **16**, 107-110 (1995).
8. Y. Wu, Z. Zhao, Y. Liu and X.G. Yang, **J. Mol. Catal. A Chem.** **155**, 89-100 (2000).
9. Z. Zhao, X. G. Yang, Y. Liu and Y. Wu, **J. Rare Earth** **16**, 325-331 (1998).
10. X.M. Yang, L.T. Luo and H. Zhong, **React. Kinet. Catal. Lett.** **81**, 219-227 (2004).
11. T.X. Cheng, X.G. Yang and Y. Wu, **Sci. China Ser. B**, **38**, 1025-1037 (1995).
12. D.C. Harris, T.A. Hewton, **J. Solid State Chem.** **69**, 182-191 (1987).
13. H. Lou, J.G. Liu, X.J. Liu and F.T. Ma, **J. Rare Earth** **19**, 324-328 (2001).
14. D. Ganguli, **J. Solid State Chem.** **30**, 353-356 (1979).
15. H. Lou, Y.Z. Xu, P. Cheng, Y.P. Ge, G.L. Lu and F.T. Ma, **Chinese J. Inorg. Chem.** **15**, 158-164 (1999).
16. Y. Tokura, H. Takagi and S. Uchida, **Nature** **337**, 345 (1989).
17. X.M. Yang, L.T. Luo and H. Zhong, **Appl. Catal. A**, **272**, 299-303 (2004).
18. L.Z. Gao, B.L. Dong, Q.S. Li, X. Lu, Z.L. Yu and Y. Wu, **J. Fuel Chem. Tech.** **22**, 113-118 (1994).
19. X.Z. Qi, Z. Ma and S.W. Wang, **Chem. Industry Engi.** **17**, 358-361 (2000).
20. Z. Zhao, X.G. Yang and Y. Wu, **Appl. Catal. B Environmental** **8**, 281-297 (1996).